Department
of
PHYSICS

UNIVERSITY OF BERGEN
Bergen, Norway

Scientific/Technical Report No. 89

ON THE DESCRIPTION OF ELECTRONIC FINAL STATES IN THE K-SHELL IONIZATION BY PROTONS.

O. Aashamar and L. Kocbach
Department of Physics, University of Bergen, Bergen, Norway.

June, 1976.

Abstract.

The choice of free electronic wavefunctions in the description of K-shell ionization by protons is discussed. The previously known discrepancies between PWBA and SCA results are shown to be entirely due to two different choices of electronic wavefunctions. Calculations in the SCA framework with Hartree-Fock-Slater wavefunctions are reported. Some general features of the SCA calculations are discussed.

1. INTRODUCTION.

It has been shown several times that the impact parameter straight line version of SCA (Semiclassical Approximation) gives total ionization cross sections equivalent to those of the PWBA (Plane Wave Born Approximation). However, numerical results reported in literature (Hansteen et al. 1975, Khandelwal et al. 1969) deviate considerably.

As a matter of fact, the explanation for this has been given many years ago by Arthurs (1959), but this work remained relatively little known. In this reference, two alternative representations for electronic final states were used in PWBA calculations. The calculated ionization cross sections for the two cases deviate in a manner similar to the deviations between the tabulated SCA and PWBA values. Since the two sets of tabulated values are obtained with alternative electronic final states, their deviations are explained by this reference.

In order to show which of the final state representations is more appropriate, we compare the tabulated cross sections to cross sections obtained using the realistic Hartree-Fock-Slater potentials (Herman & Skillman 1963) for constructing the electronic free and bound states.

In the text, results obtained with these wavefunctions are

denoted (HFS). In the tabulated SCA calculations, unmodified hydrogenic wavefunctions for screened target charge are used. The symbol chosen is (H). The modified hydrogenic wavefunction used in PWBA tables are denoted (MH). The reasons for the deviations are illustrated by means of simple physical pictures.

It is also suggested that the Figure of Arthurs is incorrect in the intermediate projectile energy region (c.f. the discussion in section 6).

The basic formulas of SCA and PWBA are reviewed in sec. 2. In section 3 the outer screening correction is discussed, while some general features of the SCA calculations are described in section 4. The results of the present (HFS) calculations and comparison with the previous approaches are found in section 5, together with a short comment on scaling relations.

2. BASIC FORMULAS.

The SCA and PWBA formulas for K-shell ionization cross sections may be expressed by means of the radial matrix elements

$$F^{\ell}_{E_f \ell, 1s}(s) = \int r^2 dr\, j_\ell(sr) R_{E_f \ell, 1s}(r) R_{i}(r) \qquad (1)$$

where $j_\ell(x)$ is the spherical Bessel function and R represents the radial wavefunctions of initial and final one electron state. For the K-shell the PWBA cross sections are expressed as

$$\frac{d\sigma}{dE_f} = 8\pi \frac{Z_1^2 e^4}{\hbar^2} \frac{M_2}{E_1} \int_{q_{min}}^{(\infty)} \sum_{\ell} (2\ell+1) \left| F^{\ell}_{E_f \ell, 1s}(s) \right|^2 \frac{ds}{s^3} \qquad (2)$$

while the corresponding straight line SCA quantity is defined through the ionization probability

$$\frac{d\sigma}{dE_f} = 2\pi \int p\, dp\, \frac{dI_p}{dE_f} \qquad (3)$$

where

$$\frac{dI_p}{dE_f} = 4 \frac{Z_1^2 e^4}{\hbar^2} \frac{M_2}{E_1} \sum_{\ell m} \left| M_p(E_f, \ell, m) \right|^2 \qquad (4)$$

Here

$$M_p(E_f, \ell, m) = \int_q^{\infty} ds\, A^{m}_{\ell}(q, p, s) F^{\ell}_{E_f \ell, 1s}(s) \qquad (5)$$

and the straight line trajectory function (Kocbach 1976)

$$A_l^m(q,p,s) = \begin{cases} \frac{2\sqrt{\pi}}{s} Y_{lm}(\cos^{-1}\frac{q}{s},0)\, J_m(p\sqrt{s^2-q^2}), & s > q \\ 0, & s < q \end{cases} \tag{6}$$

It has been shown by Amundsen (1976 - Appendix) that inserting the formulas (4) to (6) into (3) one obtains, after some simple rearrangements, exactly formula (2). This means that the straight line SCA and PWBA are equivalent.

The only difference is in q_{min} and q entering the formulas (2) and (4).

$$q \quad \frac{\Delta E}{\hbar v_i} = \frac{E_B + E_f}{\hbar v_i} \tag{7}$$

while q_{min} is found from the momentum conservation. The difference is, however, of the order m/M, i.e. negligible. An important quantity used to characterize the calculations is the ratio of adiabatic radius q_0^{-1} and the K-shell radius a_0/Z_s

$$r_{A0} = \frac{\hbar v_i}{E_B} \frac{Z_s}{a_0} \tag{8}$$

(note that the q_0 is q for $E_f = 0$). This quantity is related to the scaling variable X (*Hansteen et al. 1975*):

$$r_{A0} = (0.079\, X)^{-1}$$
$$X = \frac{Z_s\, \theta}{\sqrt{[E_i]}} \tag{9}$$

where $[E_1]$ is the magnitude of projectile energy measured in MeV, and

$$\Theta = \frac{E_B}{Z_s^2 R_\infty} \qquad (10)$$

The target screened atomic number Z_s is defined e.g. in (Hansteen et al. 1975). In the above formulas the index 1 refers to quantities characterizing the projectile. The scaling variable used in PWBA calculations is the squared ratio between projectile and electron velocity

$$\eta = \left(\frac{v_e}{v_1}\right)^2 = 40.06 \frac{[E_1]}{Z_s^2} \qquad (11)$$

with the same notation.

The relation between r_{A0} and η is easily seen to be

$$r_{A0}^2 \Theta^2 = 4\eta \qquad (12)$$

3. THE PROBLEM OF OUTER SCREENING.

Since the calculated quantities are strongly dependent on the energy transfer, the correct experimental ionization potential is necessarily used.

The difference between the experimental and hydrogen-like ionization potential $Z_s^2 R_\infty$ is usually characterized by Θ, eq.(10) which ranges from .6 for light atoms to 1. When the simple hydrogenic bound states are used to describe the

states of an atomic electron, this difference in energies should be taken into account.

In the SCA calculations, the procedure adopted is to correct for $\Theta \neq 1$ only by inserting the experimental ionization potential (Burr and Bearden 1967) into the expression for q, eq. (7). It means that the continuum states corresponding to electron final energy $E_f = \hbar^2 k^2/2m$ are the Coulomb waves with asymptotic wave number k. This choice is denoted (H). The same choice has been made in works on photoionization, quoted by Arthurs (1959) as (MMS).

In the PWBA calculations, another procedure has been adopted. The energy difference between $Z_s^2 R_\infty$ and the experimental ionization potential E_B is known to be caused by interaction with the outer shell electrons. The nature of the procedure may be understood from the Hartree-Fock description. The potential felt by the electrons is plotted in Figure 1(a) and compared with the potential $-\frac{Z_s e^2}{r}$. It is seen that in the K-shell space region $\left(\lesssim \frac{a_0}{Z}\right)$ the realistic potential approaches $-\frac{Z_s e^2}{r} + V_s$ where V_s is a positive constant. Thus, the realistic negative energy solution must behave as a solution in $-\frac{Z_s e^2}{r}$ since this represents only a shift in energy scale. In the $-\frac{Z_s e^2}{r} + V_s$ potential, the continuum threshold lies at an energy $Z_s^2 R_\infty$ above the bound state, i.e. shifted by $V_s = Z_s^2 R_\infty - E_B$ from the real continuum threshold of the realistic potential. In the K-shell

region, the realistic continuum states near the real threshold would thus behave as states with negative energy $-V_s$ in the potential $-\frac{Z_s e^2}{r} + V_s$. This may be visualized considering construction of these states by numerical outward integration.

The states with negative continuum energy in Coulomb potential are obtained by analytic continuation of the Coulomb continuum waves to the region of imaginary k. Naturally, such states behave unphysically for large distances. However, as follows from the above discussion, they should be a good approximation to the proper wavefunctions in the region where the realistic potential is well approximated by energy-shifted Coulomb potential. A similar discussion is found in (Merzbacher and Lewis 1958, section 4).

Numerical calculations with such functions might be difficult due to their diverging tails. Fortunately, the evaluation of PWBA quantities is carried out analytically so far, that the described procedure reduces to inserting imaginary k's in a comparatively simple analytic expression. The special advantage to be mentioned is that the standard PWBA calculations do not use the partial wave expansion, as the SCA. Applying this procedure in the SCA formalism is thus less straight forward and has not been attempted.

Instead, we have solved the radial equation for Hartree-Fock-Slater potential and used the resulting wavefunctions

for evaluating the functions $F^{\ell}_{fi}(s)$, eq.(1). The (HFS) wavefunctions are compared with the unmodified hydrogenic wavefunctions (H) in Figure 2. The resulting functions $F^{\ell}_{fi}(s)$ for states near threshold are compared in Figure 3(a). Their deviations may be understood from Figures 1 and 2, as discussed below.

4. SOME GENERAL FEATURES OF SCA CALCULATIONS.

Some qualitative features of the SCA results may be understood from the behaviour of the functions $F^{\ell}_{fi}(s)$. As seen from the PWBA formula (2) and the Figure 3(a), the contributions to the total cross section with $\ell = 0$ and $\ell = 1$ are always dominating for $q_o r_K > 1$ ($q_o r_K = 1$ corresponds to $\frac{\eta}{\Theta^2} = .25$). Thus including only $\ell = 0$ and $\ell = 1$ final electron states should be a good approximation in this energy region. Further, it can be seen that for decreasing projectile energy the $\ell = 0$ dominates, as known previously.

The relative contributions to the total cross section of terms corresponding to different final state ℓ are compared in Figure 4. This figure is prepared on the basis of the usual SCA calculations (H), Hansteen et al. (1975).

In this connection, it might be interesting to investigate the impact parameter distribution of these contributions.

As an example the SCA (H) calculation for 30 keV protons on carbon ($q_0 r_K = 1.67$) is used. From Fig. 4 one sees that the $\ell = 1$ contribution is about 65 per cent of the $\ell = 0$ term. The Fig. 5 shows that for impact parameter ~ 0, the $\ell = 0$ contribution to ionization probability I_p is relatively much lower, about 30 per cent, of the $\ell = 0$ contribution. However, for large impact parameters, the $\ell = 1$ term for I_p dominates.

This may be related to a simple physical picture. It is less probable to eject an electron with nonzero angular momentum from the vicinity of the center. This can be related to the centrifugal barrier, shown in Fig. 1(b).

Since the influence of centrifugal barrier is slightly different for the (H) and (HFS) cases, some of the difference between the two calculations can be understood from this picture. This is discussed further in section 5.

In the derivation of the SCA scaling relations (Karmaker and Kocbach 1973, Kocbach 1976) it has been assumed that $F^{\ell}_{fi}(s)$ is independent of the final state energy. In Fig. 3(c), the $F^{0}_{1s_0,1s}(s)$ are plotted for several final energies E_f. For large values of s these functions nearly coincide. This explains why the scaling relations are nearly exactly valid for low energy region (both (H) and (HFS)). Detailed comparison of Fig. 3(a) and (b) would

show that for $\ell > 0$ the $F_{fi}(s)$ functions do not coincide for different final energies. However, with the (H) wavefunctions, the approximate validity of the scaling relations has been confirmed empirically with small deviations (Hansteen et al. 1975, table II, correction factors).

It should be emphasized that these scaling relations are only a property of the calculations with the unmodified hydrogenic wavefunctions (H). For the two other cases, they are valid only in the very low projectile energy region (cf. Fig.7).

5. COMPARISON OF THE NUMERICAL RESULTS.

We have chosen two cases, carbon and copper for numerical calculations. Total ionization cross sections obtained from SCA (H) (Hansteen et al. 1975), PWBA (MH) (Khandelwal et al. 1969) and SCA (HFS) (present work) calculations are compared in Fig. 6. This should only represent a comparison between the three approaches to the wavefunctions since, as stated before, PWBA and SCA should give identical results.

From the cross section curves, one can see that the results with (MH) convention agree closely with the (HFS) calculations. The 5 - 10% deviation is in agreement with the conclusions of Basbas and Khandelwal (1966) (reported in Fig. 4 of Basbas et al. 1973). In that case, the (MH) and (HFS) wavefunctions were both used in (PWBA) calculations.

The SCA results with unmodified hydrogenic functions (H) coincide with the (HFS) results at low energies, as seen in the carbon part of Fig. 6. This can be related to Fig. 3(a) where for large s the two matrix elements for $\ell = 0$ coincide. For low energies, the $\ell = 0$ dominates, as is shown in Fig. 4. In the projectile energy region where $\ell = 1$ contributions become more important (c.f. Fig. 4), the (H) results lie slightly above the (HFS) results. The plot of F_{fi}^{1} is in agreement with this behaviour, even if the manifestation of this effect is not so transparent. In section 4, the role of centrifugal barrier was mentioned. It follows (Fig. 1 b, c) that the ejection of an electron with $\ell \geq 1$ from the inside of the K-shell is less probable in the (HFS) case. Thus, for intermediate energy collisions where the inside of the K-shell still contributes most, but $\ell \geq 1$ becomes important, the (HFS) result should be smaller than the pure Coulomb (H). In the projectile high energy region, the (HFS) results become higher than pure Coulomb (H). This behaviour may be again traced back to Fig. 3.

For carbon, $\Theta = .64$, for copper $.8$. The two cases were chosen to show Θ-dependence of the effects. As expected, the effects are more apparent for Θ further away from unity.

As discussed above, the SCA with hydrogenic wavefunctions (H) scales nearly exactly according to

$$F(X) = \theta Z_s^4 \sigma_K$$
$$X = \frac{Z_s \theta}{\sqrt{[E_i]}} \qquad (13)$$

Thus the SCA total cross sections, up to small corrections, may be obtained from the $\theta = 1$ PWBA calculations. To demonstrate that the $\theta \sim 1$ PWBA calculations behave as the SCA (H) calculations, we have plotted in Fig. 7 directly the tabulated values of Khandelwal et al. (1969) for $\theta = .95$ (which is the nearest to 1. published) and two other cases. The tabulated values are multiplied by appropriate factors and plotted as functions of $\eta\, \theta^{-2}$ (cf. eqs. (11) and (12)) according to equation (13). The similarity with Fig. 6 is obvious.

The increase of scaled ionization cross sections with increased outer screening (smaller θ) in the projectile high velocity region has been remarked previously (Merzbacher, Lewis 1958, Arthurs 1959). To our knowledge, the inverse behaviour in the intermediate energy region has not been discussed. In the paper of Arthurs (1959), Fig. 1, the curves even do not cross (cf. Fig. 7), but join. It is suggested that Arthurs' figure is incomplete, since both our results (Fig. 6), the tables of PWBA results (Fig. 7) and the argument given below support the crossing of the curves.

To investigate the latter deviations, we have again plotted ionization probabilities for the same case as in Fig. 5.

However, here we compare the ionization probabilities for (H) and (HFS) cases. The plot of pI_p shows that the deviation comes mostly from the large impact parameter region. From Fig. 5 we conclude that this is caused by the difference in $\ell \geq 1$ contributions. As discussed above, this may be related to the increased role of centrifugal barrier in the (HFS) potential.

6. CONCLUSION

The discrepancies between the SCA and PWBA calculations were shown to originate from the different treatment of continuum states in the published calculations. The SCA calculations with realistic continuum wavefunctions agree very well with the PWBA calculations with modified hydrogenic wavefunctions. This confirms the previously announced result (Basbas and Khandelwal 1966) and shows that the modified hydrogenic states are a good representation of the continuum in the treatment of the K-shell ionization. It should be noted that recent investigations of the L-shell case (Choi 1975) show that this approximation is not entirely so successful. This may be related to the discussion in section 3. The unphysical behaviour of the modified hydrogenic functions for large distances influences probably the result in this case. Besides, the assumption that the screening potential is constant in the whole region relevant for the L-shell contradicts the assumption that this is the case for the

K-shell. However, they are always better than those used in the SCA tables.

In the region of projectile energies most often studied ($.1 < \eta < 1.$ or $20 > x > 7$), the results of calculations with realistic wavefunctions lie below the standard SCA results (Hansteen et al. 1975, Mosebekk etc.).
A comparison of the ionization probabilities for these two calculations show that the difference is mostly due to contributions from large impact parameters. This improves the agreement between experiment and theory, since the standard SCA calculations were known to overestimate ionization probability for large impact parameters (Lægsgaard et al. 1972).

The authors would like to thank professor J. M. Hansteen for his interest in this work and P. A. Amundsen for many discussions and suggestions. To J. U. Andersen, E. Lægsgaard and K. Taulbjerg we are indebted for general discussions on the experimental results and the scaling relations.
One of us (O. A.) would like to acknowledge the financial support from the Norwegian Council for Science and the humanities (NAVF).

REFERENCES.

Amundsen P.A. (1976) J. Phys.B: Atom. Molec. Phys. 9, 971-83.

Arthurs A.M. (1959) Proc. Phys. Soc. 73 681-84.

Basbas G. and Khandelwal G.S. (1966) Bull. Am. Phys. Soc. 11 307.

Basbas G., Brandt W. and Laubert R. (1973) Phys. Rev. A7 983-1001.

Bearden J.A. and Burr A.F. (1967), Rev. Mod. Phys. 39 125-142.

Choi B.H. (1975) Phys. Rev. A 11 2004-10.

Hansteen J.M., Johnsen O.M. and Kocbach L. (1975) At. Data and Nucl. Data Tables 15 305-17.

Herman F. and Skillman S. (1963) Atomic Structure Calculations (Prentice-Hall, Englewood Cliffs, New Jersey).

Karmaker R. and Kocbach L. (1973) Sci./Tech. Report No. 58, Dept. of Physics, University of Bergen.

Khandelwal G.S., Choi B.H. and Merzbacher E. (1969) Atomic Data 1 103-20.

Kocbach L. (1976) J. Phys. B: Atom. Molec. Phys. in print.

Lægsgaard E., Andersen J.U. and Feldman L.C. (1972) Proc. Int. *Conf. on Inner Shell Ionization Phenomena and Future* Applications, Atlanta Georgia, ed. R.W. Fink et al. (Oak Ridge: USAEC) 1019-35.

Merzbacher E. and Lewis H.W. (1958) Hand. Phys. 34 (Springer Verlag, Berlin) p. 166.

FIGURE CAPTIONS.

Fig. 1 Comparison of Hartree-Fock-Slater potential (Herman & Skillman 1963) for copper with the Coulomb potential $-Z_s e^2/\rho$. Centrifugal terms for indicated ℓ-values are included.

Fig. 2 Some examples of continuum radial wavefunctions obtained for potentials shown in Fig. 1. Full lines (HFS) functions, dashed lines unmodified hydrogenic functions (H). The indicated electron energies are given in units of $Z_s^2 R_\infty$.

Fig. 3 The radial integrals $F^{\ell}_{E_f \ell, 1s}(s)$, eq. (i).

(a) Low final electron energy. Comparison of the (HFS), full line, and (H), dashed line for indicated ℓ-values.

(b) (HFS) functions for higher electron energy. Illustration of E_f and ℓ-dependence. The higher ℓ-values relatively more important than for (a).

(c) Functions $F^{0}_{E_f 0, 1s}(s)$ for three different electron final energies.

Fig. 4 SCA calculations of K-shell ionization total cross sections (Hansteen et al. 1975), (H) wavefunctions. The relative importance of terms with different ℓ-values is illustrated.

Fig. 5 Final electron ℓ contributions to the K-shell ionization probability as functions of impact parameter. The SCA (H) calculation for 30 keV protons on carbon. This result can

be scaled to about 1.18 MeV protons on copper.

Fig. 6 Total cross sections for proton impact on carbon and copper. The dotted line shows PWBA results taken from tables of Khandelwal et al. (1969). Full line and dashed line represent SCA calculations with (HFS) and (H) functions, respectively.

Fig. 7 PWBA K-shell ionization cross section functions tabulated by Khandelwal et al. (1969) scaled according to the SCA scaling, eq. (13), for three different θ-values.

Fig. 8 The ionization probability I_p (curves ①) and pI_p (curves ②) for 30 keV protons on C plotted as functions of impact parameter. Full line: (HFS) wavefunctions, dashed line (H) wavefunctions. Curves ② are in arbitrary units.

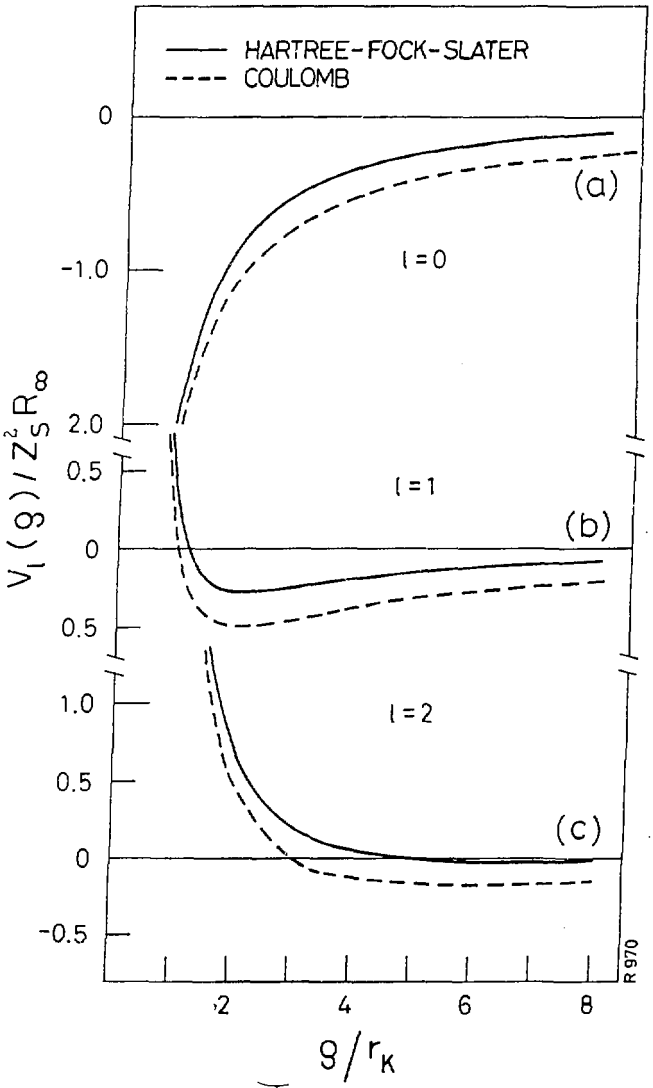
HARTREE-FOCK-SLATER
COULOMB
0
-1.0
2.0
0.5
0
0.5
1.0
0.5
0
-0.5
(a)
l = 0
l = 1
(b)
l = 2
(c)
$V_l(g) / Z_S^2 R_8$
2
4
6
8
g / r_K
R 970

Fig. 1

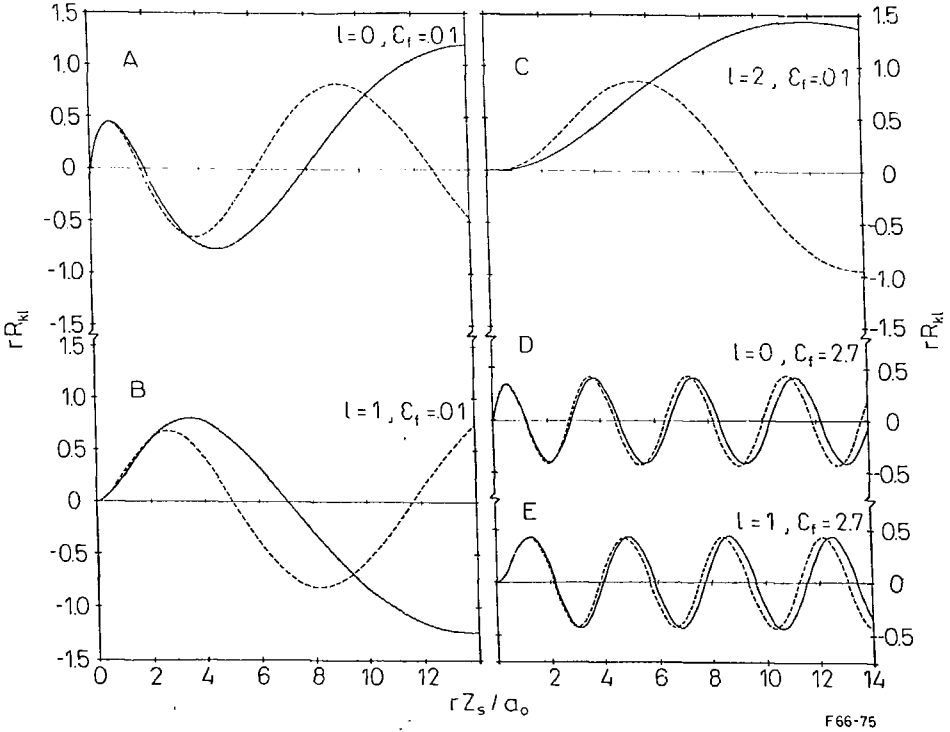
A
l = 0 , ζ_f = 0.1
B
l = 1 , ζ_f = 0.1
C
l = 2 , ζ_f = 0.1
D
l = 0 , ζ_f = 2.7
E
l = 1 , ζ_f = 2.7
rR_{kl}
rZ_s / a_o
F66-75

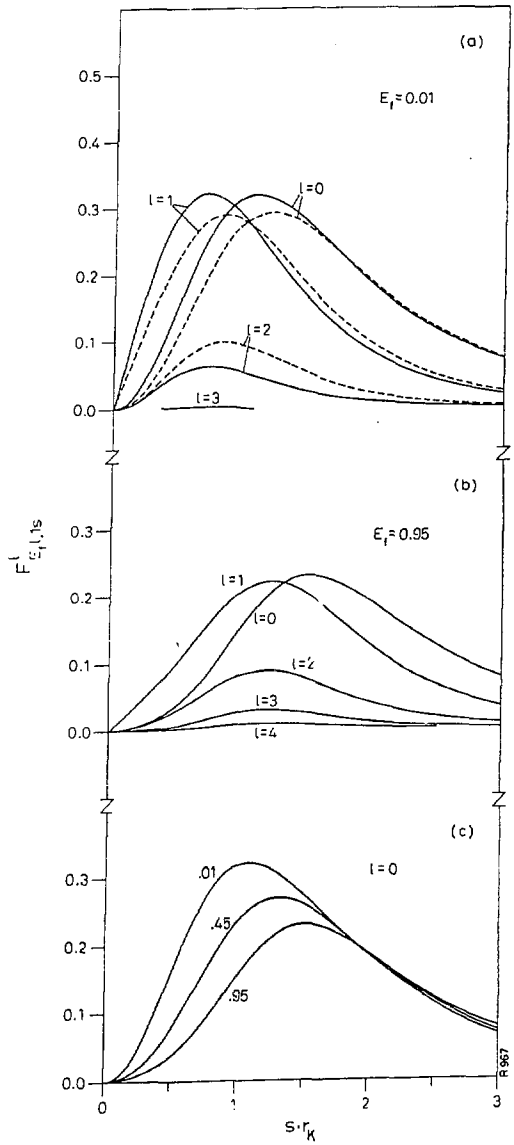
(a)
$E_f = 0.01$
l=1
l=0
l=2
l=3
(b)
$E_f = 0.95$
l=1
l=0
l=2
l=3
l=4
(c)
l=0
.01
.45
.95
$F^l_{E_f,l,s}$
$s \cdot r_K$
R 967

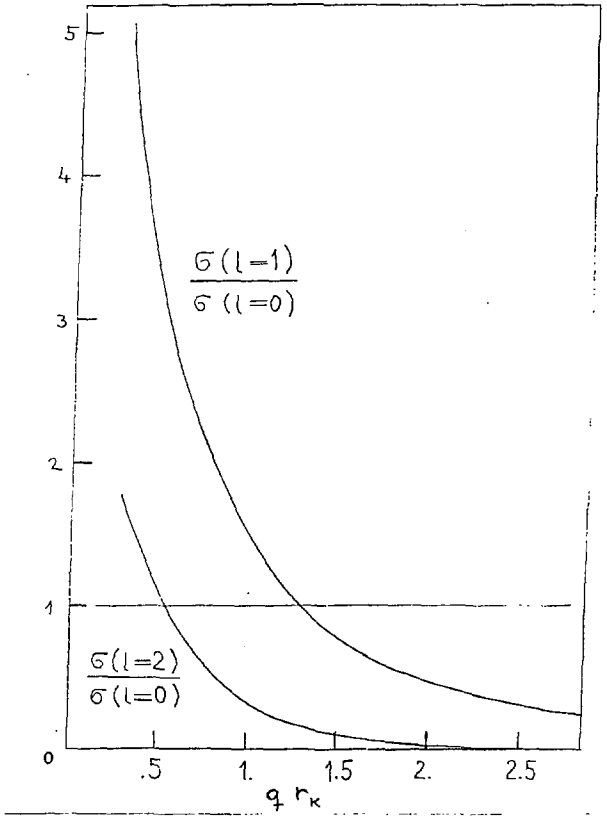

Fig. 1

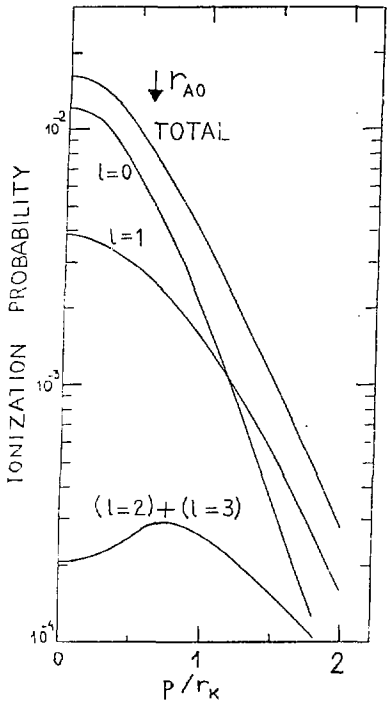
r_{A0}
TOTAL
l=0
l=1
(l=2)+(l=3)
IONIZATION PROBABILITY
10^{-2}
10^{-3}
10^{-4}
0
1
2
P/r_K

Fig. 5

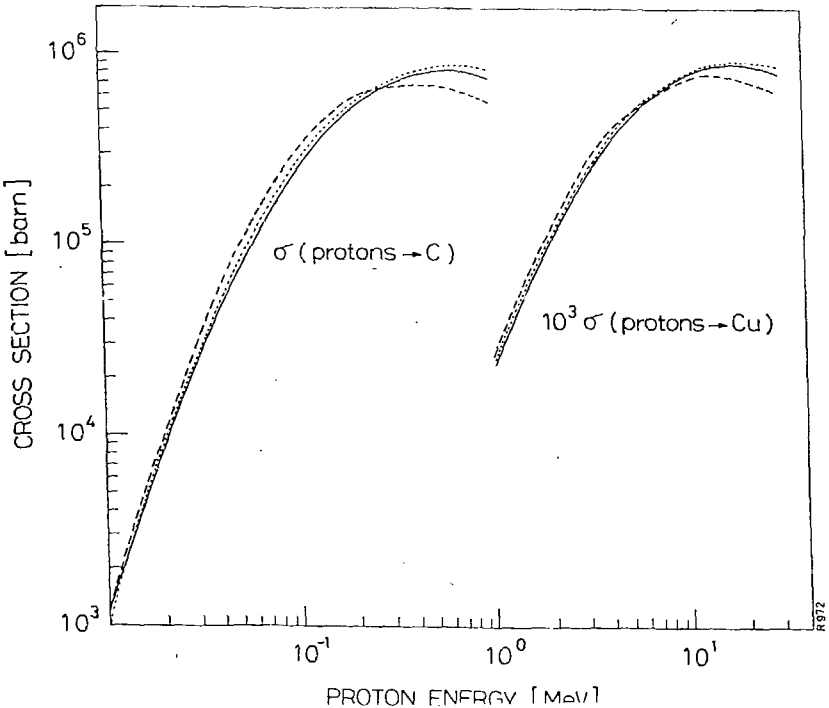
CROSS SECTION [barn]
10^6
10^5
10^4
10^3
σ (protons → C)
$10^3\,\sigma$ (protons → Cu)
10^{-1}
10^0
10^1
PROTON ENERGY [MeV]
R972

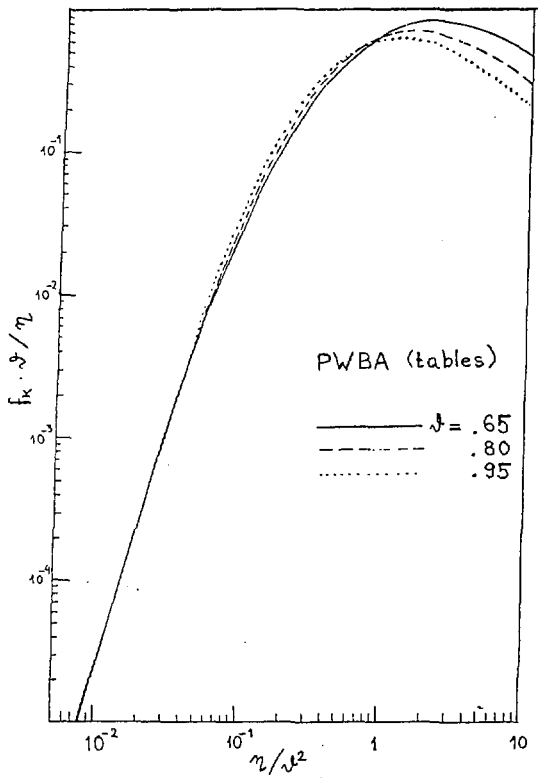
PWBA (tables)
ϑ = .65
.80
.95
$f_K \cdot \vartheta / \eta$
η / ϑ^2
10^{-2}
10^{-1}
1
10

Fig. 4

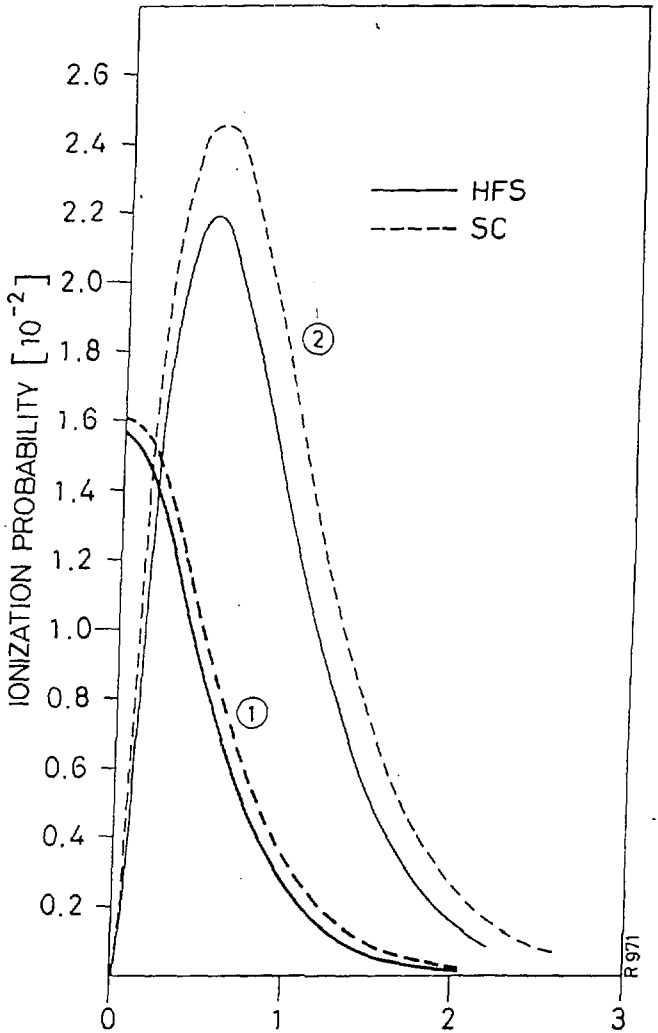
2.6
2.4
2.2
2.0
1.8
1.6
1.4
1.2
1.0
0.8
0.6
0.4
0.2
IONIZATION PROBABILITY [10^{-2}]
HFS
SC
①
②
0
1
2
3
IMPACT PARAMETER / r_K
R 971

Fig. 2